UC Davis
UC Davis Previously Published Works

Title

The spindle assembly function of Caenorhabditis elegans katanin does not require microtubule-severing activity

Permalink

https://escholarship.org/uc/item/5v26f7kj

Journal

Molecular Biology of the Cell, 22(9)

ISSN

1059-1524

Authors

McNally, Karen Perry
McNally, Francis J

Publication Date

2011-05-01

DOI

10.1091/mbc.e10-12-0951

Peer reviewed

The spindle assembly function of *Caenorhabditis elegans* katanin does not require microtubule-severing activity

Karen Perry McNally and Francis J. McNally
Department of Molecular and Cellular Biology, University of California, Davis, Davis, CA 95616

ABSTRACT Katanin is a heterodimeric microtubule-severing protein that is conserved among eukaryotes. Loss-of-function mutations in the *Caenorhabditis elegans* katanin catalytic sub-unit, MEI-1, cause specific defects in female meiotic spindles. To determine the relationship between katanin's microtubule-severing activity and its role in meiotic spindle formation, we analyzed the MEI-1(A338S) mutant. Unlike wild-type MEI-1, which mediated disassembly of microtubule arrays in *Xenopus* fibroblasts, MEI-1(A338S) had no effect on fibroblast microtubules, indicating a lack of microtubule-severing activity. In *C. elegans*, MEI-1(A338S) mediated assembly of extremely long bipolar meiotic spindles. In contrast, a nonsense mutation in MEI-1 caused assembly of meiotic spindles without any poles as assayed by localization of the spindle-pole protein, ASPM-1. These results indicated that katanin protein, but not katanin's microtubule-severing activity, is required for assembly of acentriolar meiotic spindle poles. To understand the nonsevering activities of katanin, we characterized the N-terminal domain of the katanin catalytic subunit. The N-terminal domain was necessary and sufficient for binding to the katanin regulatory subunit. The katanin regulatory subunit in turn caused a dramatic change in the microtubule-binding properties of the N-terminal domain of the catalytic sub-unit. This unique bipartite microtubule-binding structure may mediate the spindle-pole assembly activity of katanin during female meiosis.

INTRODUCTION

Katanin was first purified from sea urchin eggs based on its ATP-dependent, microtubule-severing activity (McNally and Vale, 1993). Katanin is a heterodimer consisting of a catalytic subunit and a regulatory subunit (McNally and Vale, 1993; Hartman *et al.*, 1998). The katanin catalytic subunit is a member of a family of closely related AAA ATPases which also includes the microtubule-disassembly proteins spastin and fidgetin. These proteins play roles in a number of diverse cellular processes, including cell divi-sion, cilia biogenesis, deflagellation, and neurogenesis (Roll-Mecak and McNally, 2010).

In *Caenorhabditis elegans*, the katanin catalytic subunit, MEI-1, is essential for meiotic spindle function (Mains *et al.*, 1990) but is destroyed by a ubiquitin-dependent pathway before assembly of the first mitotic spindle (Pintard *et al.*, 2003). The MEI-1(P99L) mu-tant protein does not bind its cognate ubiquitin ligase (Pintard *et al.*, 2003), and therefore persists on the first mitotic spindle (Clark-Maguire and Mains, 1994a), resulting in embryonic lethality due to defective mitosis (Mains *et al.*, 1990). Genetic screens for suppres-sors of this embryonic lethality have identified a large number of intragenic suppressor mutations in MEI-1 and extragenic suppressor mutations in MEI-2 (Mains *et al.*, 1990; Clandinin and Mains, 1993). These suppressor mutations all reduce the ectopic activity of MEI-1(P99L) during mitosis but otherwise fall into two classes.

Mutants in the first class, including the null allele, *mei-1(P99L;ct101)*, are 100% maternal-effect embryonic lethal as ho-mozygotes. *mei-1(null)* or *mei-2(null)* meiotic spindles consist of a disorganized mass of microtubules that lack the discrete parallel bundles and focused spindle poles characteristic of wild-type mei-otic spindles (Mains *et al.*, 1990; Yang *et al.*, 2003). Because of

these spindle defects, the chromosomes in a *mei-1(null)* or *mei-2(null)* spindle never congress or exhibit organized anaphase chromosome separation (Yang et al., 2003). Deep invaginations of the cortex result in expulsion into polar bodies of random subsets of chromosomes, and none of these embryos develop to hatching (Mains et al., 1990; Yang et al., 2003).

A second class of mutation includes alleles like *mei-1(P99L;P235S)* that, when homozygous, result in low rates of embryonic lethality, suggesting that meiotic spindles are functional (Mains et al., 1990). Of these homozygous viable suppressors of *mei-1(P99L)*, the *mei-2(A237T)* mutant has been characterized in the greatest detail. In contrast with *mei-1(null)* spindles, *mei-2(A237T)* meiotic spindles are bipolar and mediate anaphase chromosome segregation (McNally et al., 2006). *mei-2(A237T)* spindles are longer than wild-type spindles during metaphase, suggesting that reduced microtubule-severing activity leads to longer spindles. After activation of the APC ubiquitin ligase, wild-type meiotic spindles first shorten in the pole–pole axis as microtubule density increases. This early shortening occurs normally in *mei-2(A237T)* spindles. Wild-type spindles then rotate to a perpendicular orientation at the cortex and continue shortening as microtubule density decreases. *mei-2(A237T)* spindles do not rotate or shorten during this phase, but microtubule density still decreases (McNally et al., 2006). These results revealed a role for katanin in regulating spindle length during metaphase and in the second phase of spindle shortening. The effect on postrotation spindle shortening suggested that MEI-1/MEI-2 might sever microtubules at spindle poles, thus causing the spindle to transform into a cylindrical shape during late anaphase.

There are two distinct models that could explain the phenotypic differences between *mei-1(null)* or *mei-2(null)* spindles and *mei-2(A237T)* spindles. In the first model, katanin's only in vivo function is to sever microtubules, and different mutations cause quantitative reductions in microtubule-severing activity. Homozygous viable mutations like *mei-2(A237T)* reduce severing activity to a level that does not interfere with mitotic spindle function but allows assembly of a long, bipolar, meiotic spindle that does not exhibit postrotation spindle shortening. Further reduction in severing activity leads to a failure in the assembly of meiotic spindle poles and parallel microtubule bundles. It is difficult to explain why microtubule-severing activity would be absolutely required for the assembly of spindle poles and parallel microtubule bundles. In the second model, some in vivo functions of katanin, like regulation of metaphase spindle length, are mediated by microtubule-severing activity, whereas other functions, such as spindle pole assembly, are mediated by different biochemical activities of katanin.

We reasoned that a separation-of-function allele of *mei-1* that eliminated microtubule-severing activity but retained spindle pole–forming activity would mediate assembly of the longest bipolar spindles. In search of such a separation-of-function allele, we measured meiotic spindle lengths in a collection of homozygous viable *mei-1* mutants. We found that the mutant with the longest meiotic spindles also lacked microtubule-severing activity. This is the first demonstration of an essential nonsevering activity for katanin.

RESULTS

In search of a separation-of-function allele, we first assayed the MEI-1 protein expression levels of a series of homozygous-viable *mei-1* point mutants (Mains et al., 1990; Clandinin and Mains, 1993) by immunoblotting synchronized young adult worms. If MEI-1/MEI-2 had multiple activities, then any mutation causing a decrease in protein concentration, like *mei-2(A237T)* (Srayko et al., 2000), would reduce all of these activities and thus could not be used to

separate microtubule-severing activity from other functions. Of 11 homozygous viable *mei-1* mutants, only 1, *P99L;sb10*, had reduced MEI-1 protein levels (Supplemental Figure S1). Of the 10 mutants with wild-type protein levels, 6 were crossed with green fluorescent protein (GFP):tubulin-expressing worms to allow an in vivo analysis of meiotic spindle lengths. Live imaging revealed that all meiotic spindles were bipolar in embryos of worms homozygous for these six viable alleles. Wild-type meiotic spindles maintain a steady-state metaphase spindle length for 6 min before initiating APC-dependent shortening (Yang et al., 2003, 2005). Therefore, pole-to-pole spindle length measurements were made of metaphase I and metaphase II spindles from short time-lapse sequences that exhibited a constant spindle length for at least 1 min to ensure that measurements of shortening spindles were not included (Figure 1 and Table 1). A subset of spindles was monitored until they initiated spindle shortening (Figure 1A) to ensure that embryos were viable. As has been reported previously, metaphase spindle length was decreased in *mei-1(P99L)* relative to *mei-1(+)*. This observation is consistent with the interpretation that MEI-1(P99L) protein levels are increased during meiosis and that the resulting increase in microtubule-severing activity leads to a reduction in the length of spindle microtubules (Johnson et al., 2009). For each of the viable missense mutants that were characterized, both MI and MII spindle lengths were increased relative to those of *mei-1(P99L)* (Figure 1B and Table 1). For the alleles *P99L;P235S* and *P99L;A338S*, however, spindle lengths were increased to the greatest extent and were longer than those of the wild type. These results suggest that microtubule-severing activity might be decreased to some extent in each of these mutants and reduced to the greatest extent in *P99L;P235S* and *P99L;A338S*.

Ala-338, which is changed to serine in *mei-1(P99L;A338S)* is conserved not only among AAA ATPases but also in prokaryotic AAA+ enzymes like the *Escherichia coli* helicase, RuvB (Supplemental Figure S2A). Mutation of this alanine in RuvB results in a complete loss of function (Iwasaki et al., 2000). Ala-338 is within a β strand that has been referred to as "sensor I," and modeling work in *E. coli* FtsH suggests that it positions the downstream asparagine that interacts with the γ-phosphate of ATP (Karata et al., 1999, 2001). Pro-235, which is changed to serine in the *mei-1(P99L;P235S)* mutant (Clark-Maguire and Mains, 1994b), is also conserved in both AAA and AAA+ ATPases (Supplemental Figure S2B) and lies within the Walker A motif or P loop. The adjacent prolines Pro-234 and Pro-235 form a sharp turn that positions the downstream lysine which is required for ATP binding (Babst et al., 1998; Scott et al., 2005a; Roll-Mecak and Vale, 2008). Thus either of these mutations has the potential to completely eliminate ATP-dependent, microtubule-severing activity.

To test MEI-1(P99L;P235S) and MEI-1(P99L;A338S) for microtubule-disassembly activity, GFP-tagged wild-type and mutant MEI-1 proteins were coexpressed with GST:MEI-2 in *Xenopus* fibroblasts and in *Xenopus* A6 cells, and the effect on interphase microtubule arrays was assayed by anti-tubulin immunofluorescence (Figure 2A). Expression of wild-type MEI-1 sometimes resulted in microtubules with two discrete ends visible (Figure 2A, left), and sometimes resulted in microtubules still emanating from the centrosome but reduced in number (Figure 2A, right). The average fluorescence intensity of anti-tubulin staining relative to that of adjacent untransfected cells was 50% (Figure 2B), indicating a 50% reduction in polymer mass. Similar results were obtained in a control experiment using cells expressing the human MEI-1 orthologue KATNA1 and the MEI-2 orthologue KATNB1 (previously referred to as p60 and p80 katanin). GFP fluorescence intensity was used to choose cells expressing the mutant forms of MEI-1 at the same or higher expression levels as wild
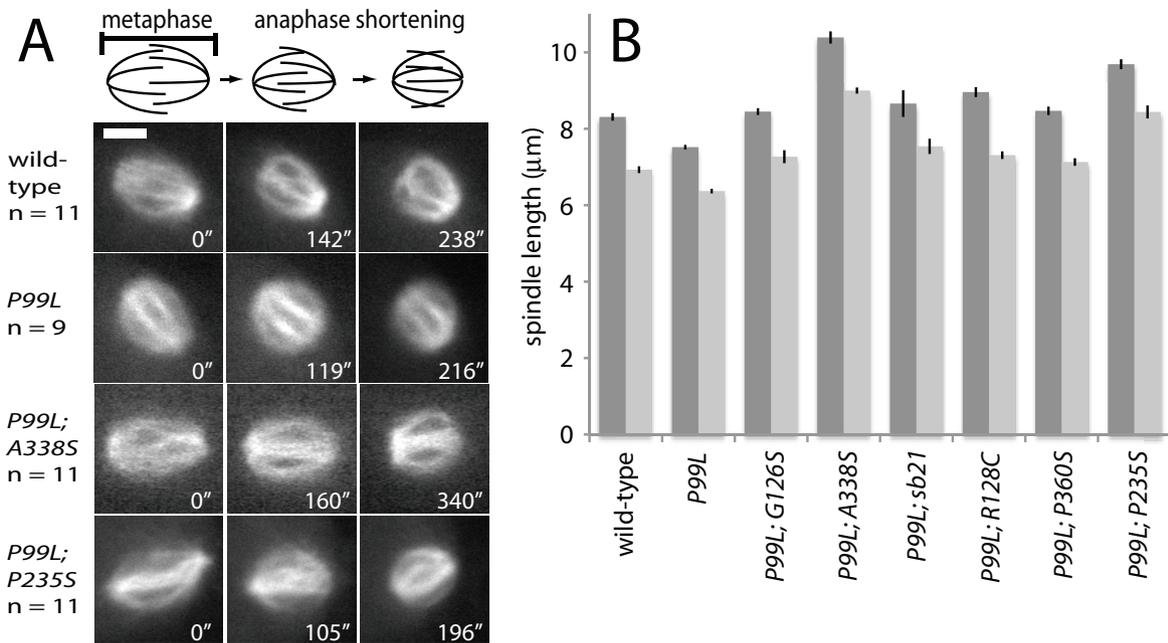
FIGURE 1: Live imaging of meiotic spindles in *mei-1* homozygous viable mutants. (A) The schematic drawing shows a metaphase meiotic spindle with microtubule bundles extending from the poles to beyond the spindle midpoint. The microtubule bundles increase in density during the initial stage of spindle shortening. Time-lapse images of worms expressing GFP:tubulin and grown at 25°C indicate that the homozygous alleles *P99L,A338S* and *P99L,P235S* result in long, bipolar spindles which undergo normal anaphase shortening. Of the spindles shown, *mei-1(P99L)* and *mei-1(P99L,A338S)* are MII; all others are MI. The line above the schematic drawing of a metaphase spindle indicates the pole-to-pole spindle length reported in B and in Table 1. Bar = 4 µm. (B) Average spindle lengths determined from time-lapse images for metaphase I spindles (dark bars) and metaphase II spindles (light bars) for the indicated *mei-1* genotypes. Error bars indicate the SE of the mean. n for each measurement is presented in Table 1.

Allele	Amino acid change	Phenotype	MI metaphase length (µm)	MII metaphase length (µm)
Wild-type, mei-1+	None	Wild-type	8.31 ± 0.10 (n = 10)	6.93 ± 0.09 (n = 10)
mei-1(ct46)	P99L	Dominant maternal effect lethal	7.52 ± 0.06 (n = 12)	6.37 ± 0.06 (n = 13)
mei-1(ct46, sb9)	P99L, G126S	Homozygous viable	8.45 ± 0.09 (n = 19)	7.27 ± 0.17 (n = 11)
mei-1(ct46, sb16)	P99L, A338S	Homozygous viable	10.39 ± 0.16 (n = 16)	9.00 ± 0.08 (n = 16)
mei-1(ct46, sb21)	N.D.	Homozygous viable	8.66 ± 0.35 (n = 14)	7.54 ± 0.20 (n = 13)
mei-1(ct46, sb22)	P99L, R128C	Homozygous viable	8.96 ± 0.13 (n = 9)	7.31 ± 0.10 (n = 14)
mei-1(ct46, sb23)	P99L, P360S	Homozygous viable	8.47 ± 0.11 (n = 14)	7.13 ± 0.10 (n = 10)
mei-1(ct46, ct103)	P99L, P235S	Homozygous viable	9.69 ± 0.13 (n = 15)	8.44 ± 0.17 (n = 12)
mei-1(ct46, ct101)	P99L, nonsense	Homozygous maternal effect lethal	No spindle poles (n = 50)	
mei-1(b284)	P225L	Homozygous maternal effect lethal	No spindle poles (n = 18)	
mei-1(ct81)	L231F	Homozygous maternal effect lethal	No spindle poles (n = 20)	
mei-1(ct46, ct82)	P99L, G473D	Homozygous maternal effect lethal	No spindle poles (n = 9)	
mei-1(ct46, ct84)	P99L, E308K	Homozygous maternal effect lethal	No spindle poles (n = 18)	
mei-1(ct46, ct89)	P99L, R414K	Homozygous maternal effect lethal	No spindle poles (n = 20)	

All other amino acid changes are from Clark-Maguire and Mains (1994b). The schematic drawing in Figure 1 shows how metaphase length was measured.

TABLE 1: Amino acid change for *sb16* was determined by sequencing two independent PCR-amplifications of the *mei-1* gene.
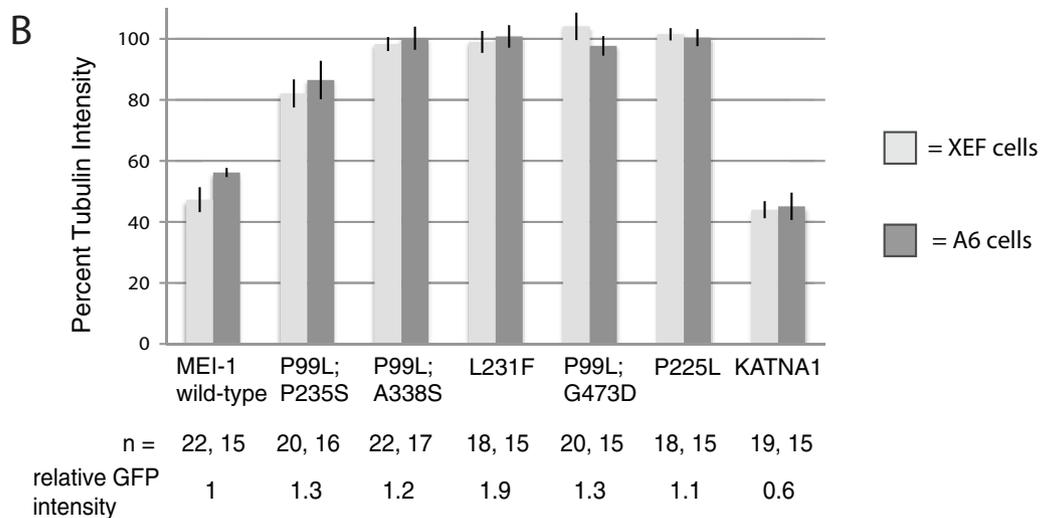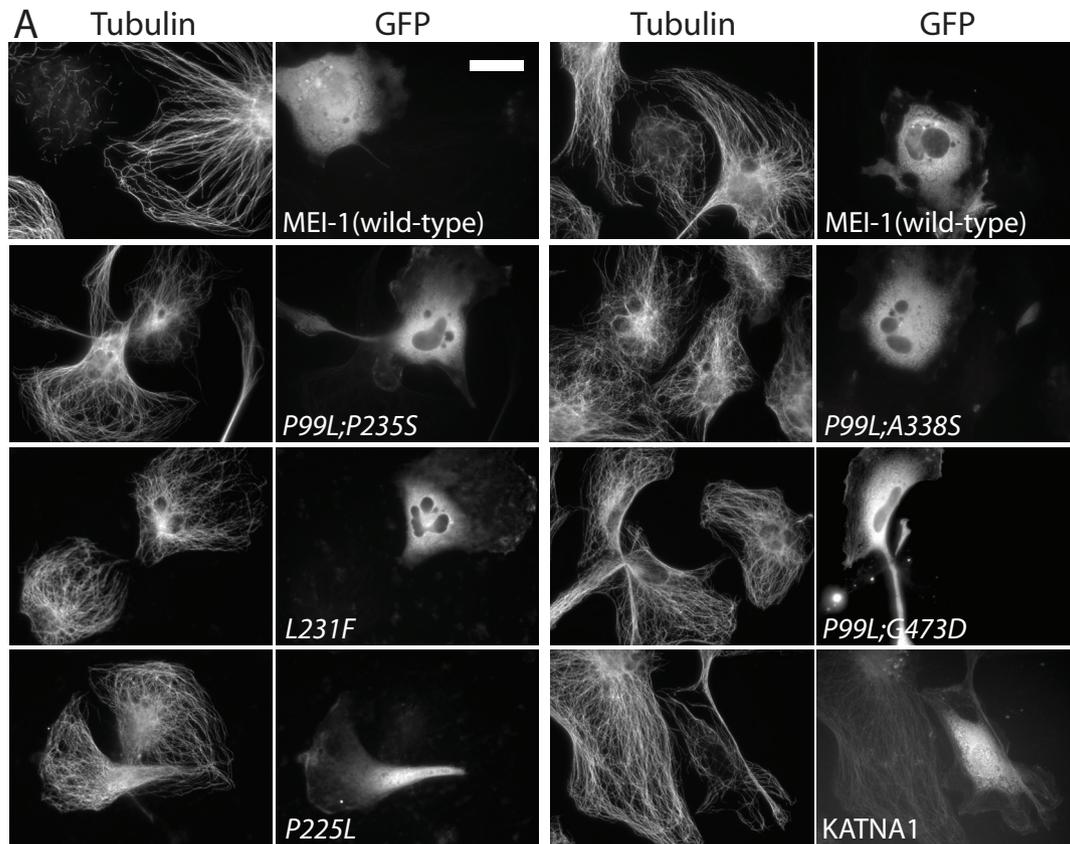
FIGURE 2: Expression of wild-type and mutant katanins in *Xenopus* tissue culture cells. *Xenopus* fibroblasts and A6 cells were cotransfected with GFP-tagged wild-type or mutant MEI-1 and with GST:MEI-2. Control cells were cotransfected with GFP-tagged human KATNA1 and with GST:KATNB1. Cells were fixed and immunostained with antibodies directed against α-tubulin, and images of high GFP expressers were captured. (A) Representative images of transfected fibroblasts. Expression of wild-type MEI-1 sometimes resulted in fragmented microtubules with both ends clearly visible (top left) but more frequently caused a reduction in the density of microtubules still emanating from the centrosome (top right) as did expression of the human homologue, KATNA1 (bottom right). Microtubule density was somewhat reduced by MEI-1(P99L,P235S). No reduction in microtubule density was seen with the homozygous viable allele, P99L;A338S, or with any of the maternal-effect lethal alleles L231F, P99L;G473D, or P225L. Bar = 25 µm. (B) Graph of relative microtubule density in transfected fibroblasts and A6 cells. For every frame captured, the average α-tubulin pixel intensity in transfected cells was expressed as a percentage of the average α-tubulin pixel intensity in adjacent nontransfected cells. Columns represent the average of the percentages for wild-type and mutant MEI-1 and KATNA1 in *Xenopus* fibroblasts (light shading) and A6 cells (dark shading). N = the number of transfected cells analyzed; bars = SEM. Relative GFP fluorescence is the average GFP pixel intensity of transfected cells for each experiment divided by the average GFP pixel intensity of wild-type MEI-1–expressing cells. A number greater than one indicates that the GFP construct was expressed at a greater level than GFP-MEI-1(wild-type).
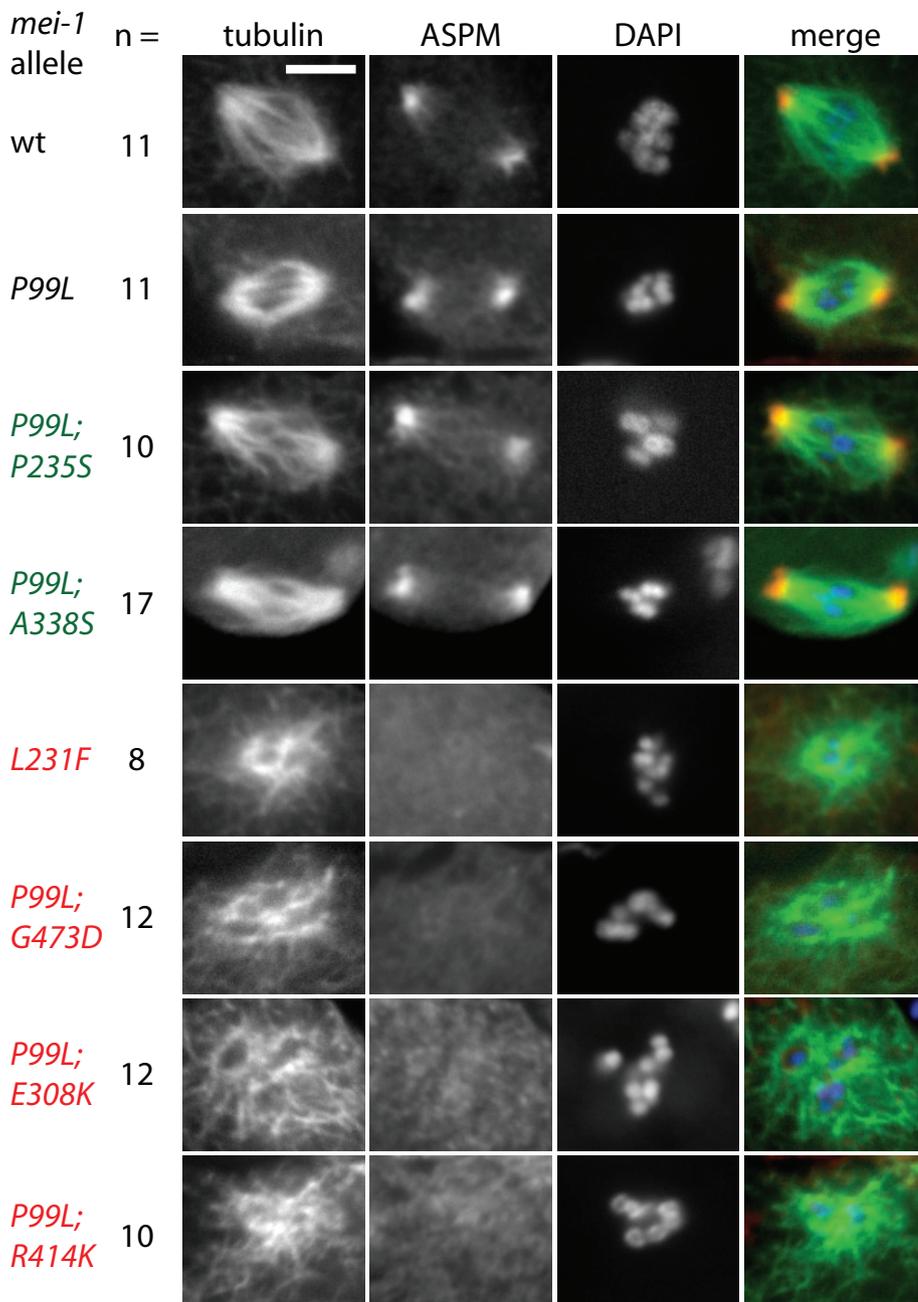
FIGURE 3: ASPM-1 immunolocalization on meiotic spindles of *mei-1* mutants. Worms were grown overnight at 25°C, and embryos were fixed and stained with antibodies directed against ASPM-1 and α-tubulin. Bipolar spindles containing a bright focus of ASPM-1 at each of two poles were present in wild-type, *P99L*, *P99L;A338S*, and *P99L;P235S* embryos. No ASPM-1 staining was observed on the meiotic spindles of the maternal-effect lethal mutants *L231F*, *P99L;G473D*, *P99L;E308K*, or *P99L;R414K*. Green alleles are homozygous viable. Red alleles are homozygous maternal-effect lethal. Each phenotype was observed in 100% of embryos of that genotype, and the number of spindles examined for each genotype is indicated. Bar = 5 μm.

loss of some other activity of MEI-1 must be responsible for the strong defect in spindle assembly previously reported for a *mei-1* null mutant and for *mei-1(RNAi)* (Mains *et al.*, 1990; Yang *et al.*, 2003).

To more carefully compare the structure of spindles assembled in the absence of MEI-1's microtubule-severing activity (P99L;A338S) with those that lack any apparent MEI-1 activity, we stained fixed meiotic embryos with antibodies specific for the spindle pole marker ASPM-1 (van der Voet *et al.*, 2009; Wignall and Villeneuve, 2009). ASPM-1 not only marks spindle poles but is required to recruit LIN-5 and cytoplasmic dynein to spindle poles (van der Voet *et al.*, 2009). Wild type, *mei-1(P99L)*, *mei-1(P99L;P235S)*, and *mei-1(P99L;A338S)* metaphase spindles all exhibited a bright focus of ASPM-1 at each of two spindle poles (Figure 3). In contrast, meiotic spindles assembled in embryos of worms homozygous for each of five homozygous maternal effect lethal alleles of MEI-1 (*L231F*, *P99L;G473D*, *P99L;E308K*, *P99L;R414K*, *ct101*) exhibited no staining of ASPM-1 on the disorganized array of microtubules associated with the chromosomes (Figures 3 and 4). The *ct101* allele is a nonsense mutant that produces no MEI-1 protein (Clark-Maguire and Mains, 1994b). *L231F* and *G473D* are mutations in highly conserved amino acids (Supplemental Figure S2, B and C; Clark-Maguire and Mains, 1994b) and have no detectable microtubule disassembly activity (Figure 2). These results show that MEI-1 protein, but not MEI-1's microtubule-severing activity, is required to assemble spindle poles.

We previously found that depletion of KLP-18, a potential microtubule cross-linker, suppressed the spindle translocation defect of *mei-1(null)* spindles (McNally *et al.*, 2006), suggesting that a spindle composed of long, cross-linked microtubules cannot translocate to the cortex. Improved confocal imaging indeed suggested that spindle microtubules are cross-linked to cytoplasmic microtubules in *mei-1(null)* embryos (Figures 3 and 4). To test whether KLP-18 depletion can rescue the spindle pole defect of *mei-1(null)* spindles, we subjected *mei-1(ct46ct101); klp-18(RNAi)* double-mutant embryos to anti-

type. MEI-1 with the P99L;P235S mutations had reduced microtubule-disassembly activity, and MEI-1 with the P99L;A338S mutations had no detectable microtubule-disassembly activity (Figure 2B). Anti-GFP immunoblots revealed that all of the GFP:MEI-1 constructs were expressed as full-length fusion proteins (Supplemental Figure S3). The result that MEI-1(P99L;A338S) had no microtubule-disassembly activity in transfected *Xenopus* cells and that this mutant allowed assembly of bipolar spindles (Figure 1) suggested that microtubule-severing activity is not required for bipolar spindle assembly and that

ASPM-1 staining. As previously reported (Wignall and Villeneuve, 2009), *klp-18(RNAi)* single-mutant embryos had a monopolar spindle with a single focus of ASPM-1 staining. Both *mei-1(null)* single-mutant embryos and *mei-1(null); klp-18(RNAi)* double-mutant embryos had no ASPM-1 staining (Figure 4). Thus MEI-1 protein, but not MEI-1's microtubule-severing activity, is directly required for spindle pole assembly.

Because *mei-1(P99L;A338S)* appeared to be a clean separation-of-function allele, we analyzed its effect on spindle rotation and on

Genotype	n=	Tubulin	ASPM	DAPI	Merge
wild-type	14				
klp-18 (RNAi)	12				
mei-1 (P99L; ct101)	10				
mei-1 (P99L; ct101), klp-18 (RNAi)	14				
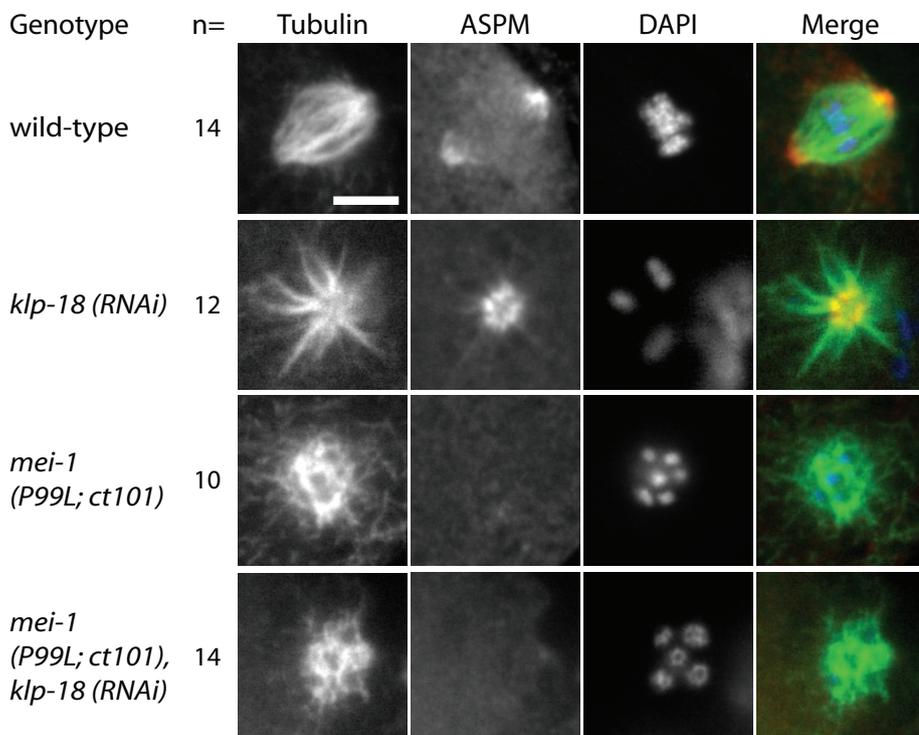
FIGURE 4: ASPM-1 is not present in meiotic spindles of *klp-18(RNAi), mei-1(null)* double mutants. Worms were grown overnight at 25°C, and embryos were fixed and stained with antibodies directed against ASPM-1 and α-tubulin. A bright ring of ASPM-1 is present at the single spindle pole in *klp-18(RNAi)* embryos, but no significant ASPM-1 staining occurs in *mei-1(P99L;ct101)* embryos or *klp-18(RNAi), mei-1(P99L;ct101)* double-mutant embryos. *ct101* is a nonsense allele of *mei-1* and behaves as a complete null (Mains *et al.*, 1990). Each phenotype was observed in 100% of embryos of that genotype, and the number of spindles examined for each genotype is indicated. Bar = 5 µm.

postrotation spindle shortening. Rotation and postrotation spindle shortening were defective in the *mei-2(A237T)* mutant (McNally *et al.*, 2006), but this mutant has a reduced amount of MEI-2 protein (Srayko *et al.*, 2000). Time-lapse imaging of GFP:tubulin revealed that both rotation and postrotation spindle shortening occurred as in wild type in the *mei-1–1(P99L;A338S)* mutant with the exception that spindle length was somewhat increased (Figure 5A). This result indicated that microtubule-severing activity is not required during these spindle stages. On the basis of the *mei-2(A273T)* phenotype, we had previously postulated that microtubule severing at spindle poles during anaphase might mediate the apparent disappearance of microtubules from outside the chromosomes. This disappearance of microtubules is significant because it has been proposed that attachments between spindle poles and chromosomes are not present during anaphase in *C. elegans* female meiotic spindles (Dumont *et al.*, 2010). To address this issue more carefully, we stained wild-type meiotic spindles with anti-ASPM-1 and found that ASPM-1–containing spindle poles are present outside the chromosomes throughout anaphase chromosome separation (Figure 5B). By both fixed immunofluorescence and improved live imaging, it is also clear that some microtubules are still present outside the chromosomes during anaphase (Figure 5, A and B). Thus the failure of *mei-2(A273T)* spindles to shorten and change in shape during anaphase is not due to a failure in severing spindle pole microtubules to place chromosomes on the end of the spindle but may reflect an altered spindle pole structure when the amount of MEI-2 protein is reduced.

What nonsevering activity of MEI-1 might mediate spindle pole assembly and ASPM-1 recruitment? Work on katanins and spastins

from other species indicates that the monomeric AAA domain can form a transient hexameric ring on ATP binding and that the ATP-bound hexamer has a higher binding affinity for microtubules than do monomers (Hartman and Vale, 1999; Roll-Mecak and Vale, 2008). X-ray structures of monomers modeled into a hexamer (Scott *et al.*, 2005a; Roll-Mecak and Vale, 2008) suggest that the N-terminal non-AAA domains extend outward from the hexameric ring. The N-terminal domains of katanin catalytic subunits from sea urchin (Hartman and Vale, 1999) and *Arabidopsis* (Stoppin-Mellet *et al.*, 2007) exhibit microtubule-binding activity suggesting that the hexameric ring might be able to cross-link six microtubules into a bundle that might lead to spindle pole formation. Furthermore, microtubule binding and bundling might be enhanced by interaction of hexameric rings with the regulatory subunits of katanin. Possible enhancement of microtubule binding by the regulatory subunit is suggested by the observations that the first 29 amino acids of the N-terminal domain of a human katanin catalytic subunit, KATNA1, are also required for binding to the regulatory subunit, KATNB1, and that KATNB1 enhances microtubule binding by KATNA1 (McNally *et al.*, 2000).

In search of nonsevering activities of MEI-1, we first tested whether the N-terminal domain is necessary and sufficient for interaction with its regulatory subunit, MEI-2. Lysates from insect cells expressing full-length MEI-1, a deletion missing the N-terminal 29 amino acids or the N-terminal domain alone were mixed with an *E. coli*–expressed maltose binding protein (MBP) fusion to MEI-2 or with MBP alone. Complexes were purified by amylose affinity chromatography, and bound complexes were analyzed by SDS–PAGE and immunoblotting. As shown in Figure 6A, the N-terminal domain was both necessary and sufficient for binding to MEI-2. Because katanin N-terminal domains had not previously been tested for binding to their corresponding regulatory subunits, we also assayed for binding of the N-terminal domain of the human katanin catalytic subunit, KATNAL1, to KATNB1, or to the previously uncharacterized homologue of KATNB1, c15ORF29 (Roll-Mecak and McNally, 2010). Like the N-terminal domain of MEI-1, the N-terminal domain of KATNAL1 was sufficient for binding both KATNB1 and c15orf29 (Figure 6B). Deletion of the N-terminal 29 amino acids of KATNAL1 had only a minor effect on binding to KATNB1 but had a stronger effect on binding to c15orf29 (Figure 6B). These results indicate that a complex between the N-terminal domain of MEI-1 and MEI-2 might be the physiologically relevant microtubule-binding structure conferring MEI-1's essential spindle pole assembly activity. Because KATB is required for KATA function in *Tetrahymena* ciliogenesis (Sharma *et al.*, 2007) just as MEI-2 is absolutely required for MEI-1's in vivo function (Mains *et al.*, 1990; Srayko *et al.*, 2000), the complex between the N-terminal domains of katanin catalytic subunits with their corresponding regulatory subunits might be generally significant.
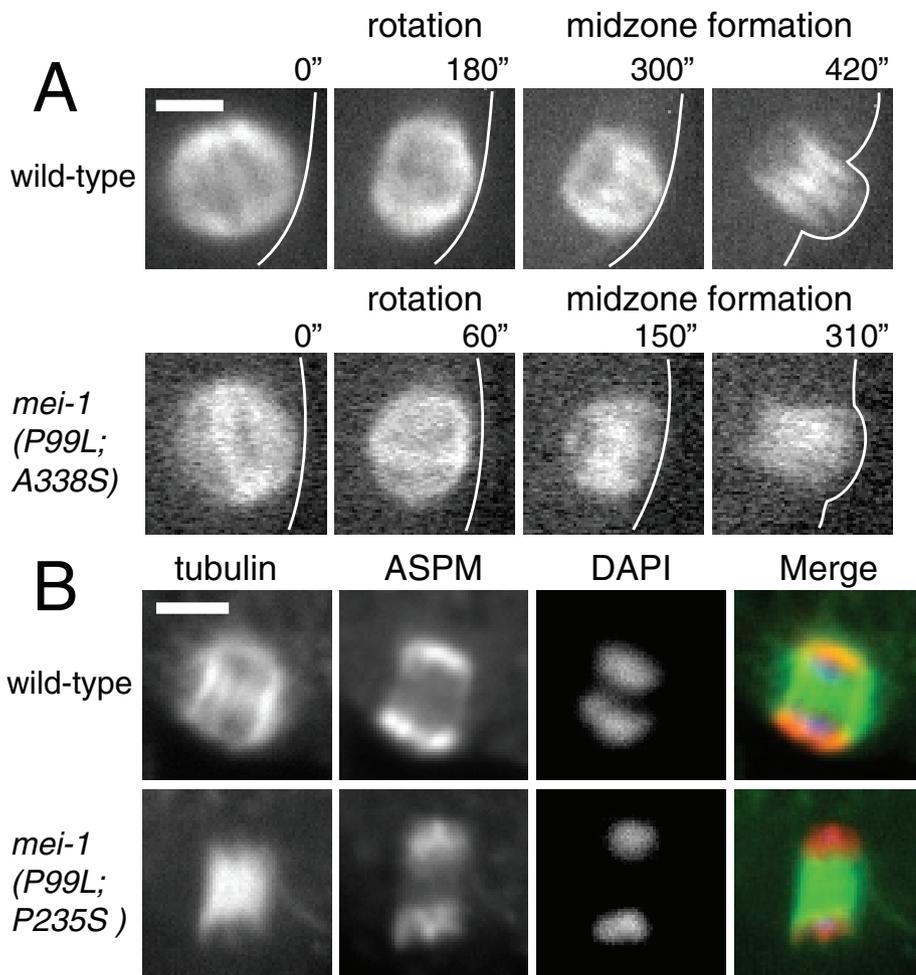
FIGURE 5: Spindle rotation and postrotation spindle shortening in *mei-1(P99L;A338S)*. (A) Time-lapse images of embryos expressing GFP:tubulin indicate that meiotic spindle rotation and postrotation shortening occurred in 7/7 *mei-1(P99L, A338S)* embryos and in 6/6 wild-type embryos. Bar = 3 µm. (B) Wild-type and *mei-1(P99L, P235S)* worms were grown overnight at 25°C, and embryos were fixed and stained with antibodies directed against ASPM-1 and α-tubulin. Wild-type embryos (22/22) and mutant embryos with anaphase meiotic spindles (10/10) had bright foci of anti-ASPM-1 staining at the spindle poles. A small amount of anti-tubulin staining was also observed at the poles in embryos with the brightest staining. Bar = 3 µm.

To investigate whether this microtubule binding is significant in vivo, a GFP fusion to the N-terminal domain of MEI-1 was co-expressed with MEI-2 in *Xenopus* fibroblasts. In the presence of MEI-2, the N-terminal domain of MEI-1 decorated a rare subset of microtubules (Figure 8). None of the full-length MEI-1 constructs assayed for microtubule-disassembly activity (Figure 2) showed any colocalization with interphase microtubules. These results indicate that the structure generated by dimerization of the MEI-1 N-terminal domain with MEI-2 can bind microtubules in vivo and that this binding is somehow inhibited in intact MEI-1/MEI-2 complexes. Exposure of the N-terminal MEI-1/MEI-2 complex may be regulated by the ATP hydrolysis cycle of the AAA domains or interactions with additional proteins in meiotic embryos.

DISCUSSION

Complexes of wild-type MEI-1 and MEI-2 sever microtubules in vitro (McNally *et al.*, 2006) and cause disassembly of interphase microtubule arrays in HeLa cells (Srayko *et al.*, 2000) and *Xenopus* fibroblasts. MEI-1(P99L; A338S) appears to lack microtubule-severing activity based on the following criteria: It has no detectable microtubule disassembly activity when expressed in *Xenopus* fibroblasts, and the mutation is in a residue conserved even in the distantly related bacterial ATPase, RuvB, where that residue is essential for function. Because our preparations of purified MEI-1(P99L;A338S) had lower protein concentration than the preparations of MEI-1(wild-type) that have robust in vitro microtubule-severing activity (McNally *et al.*, 2006), we could not use in vitro severing assays to demonstrate a lack of activity for MEI-1(P99L;A338S). In contrast, we could readily find individual *Xenopus* cells expressing GFP-MEI-1(P99L;A338S) with higher GFP fluorescence intensity than that of cells expressing GFP-MEI-1(wild-type). No individual cells expressing GFP-MEI-1(P99L;A338S) showed any discernable signs of microtubule disassembly.

Meiotic spindles assembled by MEI-1(P99L; A338S) have metaphase lengths that are significantly longer than those assembled by MEI-1(P99L; P235S), a protein with greatly reduced microtubule-disassembly activity in fibroblasts. Because the expression level of MEI-1(P99L; A338S) protein and that of MEI-1(P99L; P235S) protein are similar to wild type, these results strongly suggest that microtubule-severing activity causes a reduction in metaphase spindle length. Because the nonsevering mutant, MEI-1(P99L; A338S), mediates assembly of spindles with two ASPM-1–positive poles but a lack of MEI-1 or MEI-2 protein causes assembly of spindles containing no ASPM-1 foci, our results indicate that a complex of MEI-1 and MEI-2 mediates spindle pole assembly through a nonsevering mechanism.

Because complexes between katanin N-terminal domains with their regulatory subunit had not previously been characterized, we tested the microtubule-binding activity of these complexes in vitro and in vivo. The N-terminal domain of human KATNAL1 showed saturable binding to microtubules assembled from highly purified, microtubule associated protein (MAP)-free porcine brain tubulin with an apparent K_d of 4 µM (Figure 7). The MEI-2–like human c15orf29 also exhibited saturable binding to microtubules with an apparent K_d of 2 µM. When these proteins were combined, the apparent K_d for the N-terminal domain was modestly decreased to 0.8 µM, and the K_d for c15orf29 was decreased to 0.9 µM. The more dramatic effect was seen in the stoichiometry of binding at saturation. The N-terminal domain of KATNAL1 saturated with only 14% bound. The presence of c15orf29 increased the fraction of the N-terminal domain bound at saturation to 50%. These results indicate that the complex between the N-terminal domain and the regulatory subunit binds microtubules in a qualitatively different manner than does the N-terminal domain alone.

FIGURE 7: A complex of the N-terminal domain of KATNAL1 and c15orf29 binds microtubules in vitro. The N-terminal domain of KATNAL1 (1–213) or a MBP fusion to c15orf29 (0.6 μM of either), or a mixture of both proteins, was bound to increasing concentrations of polymerized tubulin. Microtubule-bound and unbound katanin were separated by centrifugation and quantified with anti-KATNAL1 immunoblots. Results of hyperbolic curve fits are shown. K_d = apparent equilibrium binding constant; B_{max} = fraction bound at saturation, and R^2 = quantification of how well the data fit the hyperbolic curve (with 1.0 being a perfect fit). Data for 1–213 and 1–213 + c15orf29 are combined data from two independent experiments.

FIGURE 6: The N-terminal domain of MEI-1 is necessary and sufficient for binding to MBP-MEI-2. (A) Lanes 1–3 are amylose bead–bound fractions from binding reactions containing MBP-MEI-2, whereas lanes 4–6 are equivalent control reactions containing MBP. Binding reactions contained either the MEI-1 N-terminal domain (1–198) (lanes 1 and 4), MEI-1 missing a small conserved portion of the N-terminal domain (36–475) (lanes 2 and 5), or full-length MEI-1 (1–475) (lanes 3 and 6). (B) The N-terminal domain of human KATNAL1 is necessary and sufficient for binding human MEI-2 orthologues. Lanes 1–3 are amylose bead–bound fractions from binding reactions containing MBP-c15orf29, lanes 4–6 are bound fractions containing an MBP fusion to amino acids 412–655 of human KATNB1, and lanes 7–9 are bound fractions containing MBP only. Binding reactions contained either the KATNAL1 N-terminal domain (1–213) (lanes 1, 4, and 7), KATNAL1 missing a small conserved portion of the N-terminal domain (32–490) (lanes 2, 5, and 8), or full-length KATNAL1 (1–490) (lanes 3, 6, and 9).

In other cell types, it has been proposed that spindle pole assembly requires the microtubule cross-linking activities of kinesin-14 (Goshima et al., 2005) or cytoplasmic dynein (Merdes et al., 2000). Because katanin is proposed to form a transient radial hexamer with N-terminal microtubule binding domains extending outward (Hartman and Vale, 1999; Roll-Mecak and McNally, 2010), it is possible that katanin promotes spindle pole formation by a microtubule cross-linking mechanism. Because mei-1(null) or mei-2(null) spindles lack poles, it is likely that a structure composed of both subunits mediates the essential function of katanin.

In this study, we showed for the first time that the N-terminal domain of MEI-1 is sufficient to bind MEI-2 and that the N-terminal domain of human KATNAL1 (one of three human MEI-1 orthologues) is sufficient to bind either of two human MEI-2 orthologues, KATNB1 and c15orf29. Both KATNB1 and c15orf29 copurify with KATNAL1 from human cells (Torres et al., 2009), but the relative concentrations and importance of different combinations of subunits are not known. The nuclear magnetic resonance structure of the N-terminal domain of mouse KATNAL1 revealed that it is a three-helix bundle called a microtubule interacting and transport (MIT) domain (Iwaya et al., 2010), a protein fold conserved in the N-terminal domains of VPS4 (Scott et al., 2005b) and spastin. Whereas the N-terminal domains of sea urchin (Hartman and Vale, 1999) and Arabidopsis (Stoppin-Mellet et al., 2007) katanin catalytic subunits exhibit saturable, low-affinity microtubule binding, qualitative binding assays suggested that the N-terminal domain of mouse KATNAL1 bound tubulin dimers or aggregates rather than microtubules (Iwaya et al., 2010). In this study, we found that the N-terminal domain of human KATNAL1 has saturable, low-affinity microtubule-binding activity like the equivalent domains of sea urchin and Arabidopsis katanins. Binding of the human KATNAL1 MIT domain to microtubules saturated with only 14% of the protein bound at saturation, however, possibly explaining the lack of binding reported for the mouse KATNAL1 MIT domain. The putative katanin regulatory subunit, c15orf29, bound microtubules by itself and saturated with 90% bound. Remarkably, an equimolar mixture of the KATNAL1 MIT domain and c15orf29 bound microtubules with a higher affinity than either protein alone and saturated at 50% bound. These results support a model in which binding of the katanin regulatory subunit to the catalytic subunit generates a completely new microtubule-binding structure. We suggest that this novel bipartite structure is the physiologically relevant microtubule-binding structure that may cross-link microtubules to allow spindle pole formation.
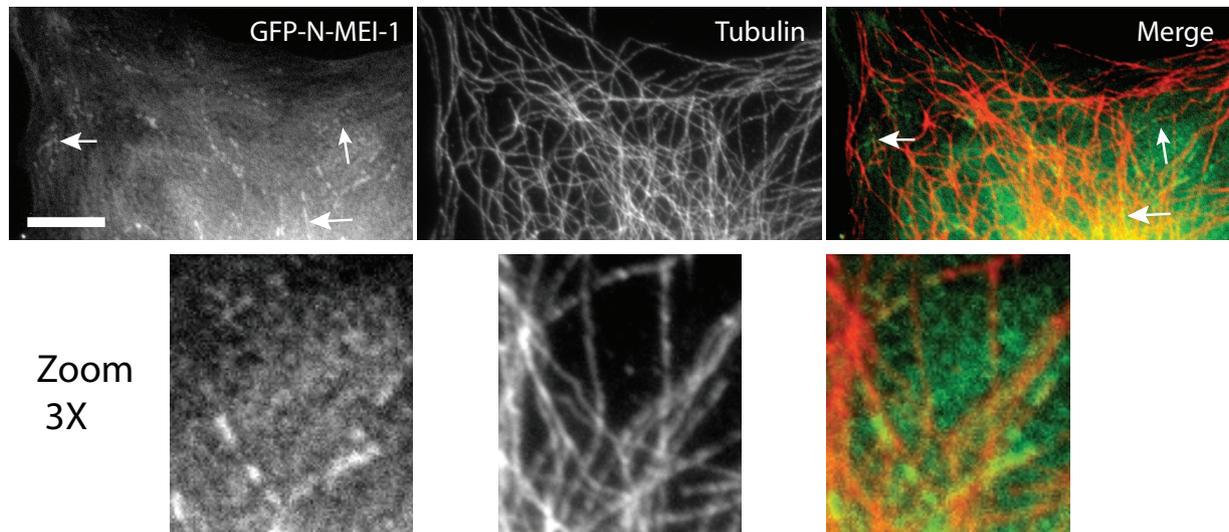
FIGURE 8: The N-terminal domain of MEI-1 binds microtubules in vivo. *Xenopus* fibroblast cells were cotransfected with a GFP fusion to the 198 N-terminal amino acids of MEI-1 and GST:MEI-2. Images of two transfected cells show tracks of GFP:MEI-1(1–198) that overlap or are interspersed with anti-tubulin staining. Arrows point to sites where individual microtubules are dotted with GFP:MEI-1(1–198). Bar = 20 μm.

MATERIALS AND METHODS

C. elegans strains
Strains were cultured according to standard procedures (Brenner, 1974). Wild type refers to AZ244 (unc-119(ed3);ruIs57[pAZ147:pie-1/β-tubulin::GFP;unc-119(+)), which is derived from N2 (Praitis *et al.*, 2001). Worms carrying the following temperature-sensitive alleles were maintained at 16°C as homozygous stocks: mei-1(ct46, sb9, sb10, sb16, sb17, sb21, sb22, sb23, ct103). Worms carrying the following nonconditional alleles were maintained as balanced heterozygous stocks: mei-1(ct81, ct82, ct84, ct89, b284). All mei-1–bearing chromosomes included an unc-13 or unc-29 mutation in *cis* to recognize the appropriate homozygous segregant. For live imaging of worms carrying temperature-sensitive mei-1 alleles, the mei-1 strains were crossed with AZ244, and progeny homozygous for mei-1, unc-13, and GFP-tubulin were isolated.

Live imaging
Adult hermaphrodite worms grown for 24 h at 25°C were anesthetized with tricaine/tetramisole (Kirby *et al.*, 1990; McCarter *et al.*, 1999) and gently mounted between a coverslip and a thin 3% agarose pad on a glass slide. Live imaging was primarily done on a Microphot SA (Nikon, Tokyo, Japan) microscope equipped with a 60× PlanApo 1.4 objective and a charge-coupled device (CCD; Qimaging Retiga Exi Fast 1394 camera). Excitation light from an HBO100 light source was attenuated with a heat- and UV-reflecting "hot mirror" (Chroma Technology, Brattleboro, VT) and a 25% transmission neutral density filter. A GFP long pass filter set (Omega Optical, Brattleboro, VT) was used. Excitation light was shuttered with a Sutter shutter controlled by a Sutter Lambda 10–3 controller and IVision software (BioVision Technologies, Exton, PA). Images shown in Figures 1 and 5A were acquired with a Perkin Elmer UltraView (Waltham, MA) spinning disk confocal microscope. All analyses were carried out using iVision software. Spindle length was measured as the distance along the pole-to-pole axis.

Plasmid constructions
The coding sequence of each protein expressed was PCR-amplified to add restriction enzyme cleavage sites and cloned into one of the

following vectors: pFastBac Dual (for baculovirus expression), pMAL-CR1 (for *E. coli* expression), pEGFP-C1 (Clontech; for expression in *Xenopus* cells). Point mutations in MEI-1 were generated by site-directed mutagenesis.

Transfection of *Xenopus* cells
Xenopus fibroblasts (provided by Vladmir Rodionov, University of Connecticut Health Center, Farmington, CT) and *Xenopus* A6 cells were grown on coverslips in 70% Leibovitz's L15 Medium supplemented with 10% fetal bovine serum and penicillin/streptomycin at 27°C. Cells were transfected with Lipofectamine 2000 using equal concentrations of GFP-MEI-1 plasmids and a GST-MEI-2 plasmid constructed in pCDNA3. Thirty-six hours after transfection, coverslips were fixed in –20°C methanol and stained with anti-tubulin antibody (DM1alpha) and Alexa594 anti–mouse secondary antibody.

Immunostaining of *C. elegans* embryos
Adult hermaphrodite worms were washed in a watch glass in 0.8× egg buffer and then transferred to a poly-L-lysine–coated Superfrost/Plus glass slide (Fisher Scientific, Pittsburgh, PA). Excess liquid was wicked away, a coverslip was gently applied, and the slides were submerged into liquid nitrogen for 10 min. Immunostaining was performed using standard freeze-fracture methods followed by –20°C methanol fixation as described previously (Tsou *et al.*, 2002; DeBella *et al.*, 2006). Primary antibodies were diluted in phosphate-buffered saline containing 0.05% Tween 20 (PBST) in the following ratios: anti-ASPM-1 (van der Voet *et al.*, 2009a), 1:100; anti-tubulin (DM1alpha), 1:200. All secondary antibodies were diluted 1:200 in PBST. The secondary antibodies used were Alexa594 anti–rabbit immunoglobulin (Ig)G (Molecular Probes, Eugene, OR) and Alexa488 anti–mouse IgG. DAPI (4',6-diamidino-2-phenylindole) staining was used to visualize DNA. Stained embryos were imaged using an Olympus (Center Valley, PA) IX71 inverted microscope equipped with a 60× PlanApo N.A. 1.42 objective, an Olympus DSU spinning disk attachment, and a Hamamatsu (Bridgewater, NJ) Orca R2 deep cooled C10600–10B digital monochrome CCD camera. Excitation light from a U-RFL-T 100W Mercury burner power supply (Olympus) was controlled by a Sutter Lambda 10–3 controller and MetaMorph

Imaging software (Universal Imaging/Molecular Devices, Sunnyvale, CA).

Protein expression and purification

E. coli BL21DE3 carrying pMAL-CR1 plasmids were grown at 18°C and induced with IPTG (isopropyl-β-D-thiogalactopyranoside) for 12 h before harvesting and lysis with a microfluidizer. Lysates were centrifuged, and supernatants were subjected to amylose affinity chromatography and eluted with 20 mM maltose. Sf9 cells were grown in SF900 serum-free medium (Invitrogen, Carlsbad, CA) in shaking flasks and infected with each virus for 48 h. Cells were harvested and lysed, and proteins were purified by Ni-chelate chromatography as previously described (McNally *et al.*, 2000).

Protein interaction assay

Amylose beads (New England Biolabs, Ipswich, MA) were incubated with excess lysate from *E. coli* expressing MBP, MBP-MEI-2, MBP-c15orf29, or MBP-KATNB1(412–655), then washed in binding buffer before addition of Ni-chelate purified baculovirus-expressed proteins. Beads were then washed in binding buffer before elution of bound proteins with SDS Laemmli buffer. Binding buffer consisted of 20 mM K-HEPES, pH 7.4, 0.4 mM EGTA, 4 mM $MgCl_2$, 0.1% Triton X-100, 1 mg/ml lysozyme, and either 400 mM KCl (for MEI-1/MEI-2) or 150 mM KCl (for human katanin). Bound proteins were detected by immunoblotting with either an anti-MEI-1 antibody or an anti-KATNA1 antibody.

Microtubule-binding assays

Ni-chelate–purified 6his-KATNAL1(1–213) (0.6 μM), 0.6 μM amylose-affinity-purified MBP-c15orf29, or 0.6 μM both proteins was incubated with increasing concentrations (0–19 μM) of paclitaxel (Taxol; Sigma-Aldrich, St. Louis, MO)-stabilized microtubules assembled from phosphocellulose-purified, MAP-free porcine brain tubulin in: 100 mM KCl, 20 mM K-HEPES, pH 7.4, 0.4 mM EGTA, 4 mM $MgCl_2$, 0.1% Triton X-100, 20 μM paclitaxel, 4 mg/ml bovine serum albumin (BSA) in a volume of 100 μl. Reactions were layered onto a 50 μl cushion of 33% glycerol in binding buffer without BSA. Reactions were centrifuged in a TL100 (Beckman Coulter, Brea, CA) fixed-angle tabletop ultracentrifuge rotor at 60,000 rpm for 10 min. Supernatants were removed, and pellets were resuspended in SDS-Laemmli buffer and analyzed by immunoblotting with an anti-KATNA1 antibody (McNally and Thomas, 1998) or an anti-MBP antibody. Signals were detected with a LI-COR (Lincoln, NE) Odyssey laser scanner, and the relative fluorescence signals in pellet and supernatant fractions were determined using iVision software. Data were fitted to hyperbolic curves using DeltaGraph. Katanin proteins were diluted into binding buffer and prespun to remove aggregates immediately before addition to microtubules. Tubulin was polymerized in a single, high-concentration batch with dimethyl sulfoxide and GTP in PME (PIPES, Mg++, EGTA) for 45 min at 37°C before the addition of paclitaxel to promote assembly of long microtubules. Microtubules were pelleted and resuspended in binding buffer immediately before the start of binding reactions. Binding reactions were carried out for 10 min at room temperature.

REFERENCES

Babst M, Wendland B, Estepa EJ, Emr SD (1998). The Vps4p AAA ATPase regulates membrane association of a Vps protein complex required for normal endosome function. EMBO J 17, 2982–2993.

Brenner S (1974). The genetics of *Caenorhabditis elegans*. Genetics 77, 71–94.

Clandinin TR, Mains PE (1993). Genetic studies of mei-1 gene activity during the transition from meiosis to mitosis in Caenorhabditis elegans. Genetics 134, 199–210.

Clark-Maguire S, Mains PE (1994a). Localization of the mei-1 gene product of Caenorhabditis elegans, a meiotic-specific spindle component. J Cell Biol 126, 199–209.

Clark-Maguire S, Mains PE (1994b). mei-1, a gene required for meiotic spindle formation in Caenorhabditis elegans, is a member of a family of ATPases. Genetics 1136, 533–546.

DeBella LR, Hayashi A, Rose LS (2006). LET-711, the *Caenorhabditis elegans* NOT1 ortholog, is required for spindle positioning and regulation of microtubule length in embryos. Mol Biol Cell 17, 4911–4924.

Dumont J, Oegema K, Desai A (2010). A kinetochore-independent mechanism drives anaphase chromosome separation during acentrosomal meiosis. Nat Cell Biol 12, 894–901.

Goshima G, Nédélec F, Vale RD (2005). Mechanisms for focusing mitotic spindle poles by minus end-directed motor proteins. J Cell Biol 171, 229–240.

Hartman JJ, Mahr J, McNally K, Okawa K, Iwamatsu A, Thomas S, Cheesman S, Heuser J, Vale RD, McNally FJ (1998). Katanin, a microtubule-severing protein, is a novel AAA ATPase that targets to the centrosome using a WD40-containing subunit. Cell 93, 277–287.

Hartman JJ, Vale RD (1999). Microtubule disassembly by ATP-dependent oligomerization of the AAA enzyme katanin. Science 286, 782–785.

Iwasaki H, Han YW, Okamoto T, Ohnishi T, Yoshikawa M, Yamada K, Toh H, Daiyasu H, Ogura T, Shinagawa H (2000). Mutational analysis of the functional motifs of RuvB, an AAA+ class helicase and motor protein for holliday junction branch migration. Mol Microbiol 36, 528–538.

Iwaya N *et al.* (2010). A common substrate recognition mode conserved between katanin p60 and VPS4 governs microtubule severing and membrane skeleton reorganization. J Biol Chem 285, 16822–16829.

Johnson JL, Lu C, Raharjo E, McNally K, McNally FJ, Mains PE (2009). Levels of the ubiquitin ligase substrate adaptor MEL-26 are inversely correlated with MEI-1/katanin microtubule-severing activity during both meiosis and mitosis. Dev Biol 330, 349–357.

Karata K, Inagawa T, Wilkinson AJ, Tatsuta T, Ogura T (1999). Dissecting the role of a conserved motif (the second region of homology) in the AAA family of ATPases. Site-directed mutagenesis of the ATP-dependent protease FtsH. J Biol Chem 274, 26225–26232.

Karata K, Verma CS, Wilkinson AJ, Ogura T (2001). Probing the mechanism of ATP hydrolysis and substrate translocation in the AAA protease FtsH by modelling and mutagenesis. Mol Microbiol 39, 890–903.

Kirby C, Kusch M, Kemphues K (1990). Mutations in the par genes of *Caenorhabditis elegans* affect cytoplasmic reorganization during the first cell cycle. Dev Biol 142, 203–215.

Mains PE, Kemphues KJ, Sprunger SA, Sulston IA, Wood WB (1990). Mutations affecting the meiotic and mitotic divisions of the early Caenorhabditis elegans embryo. Genetics 126, 593–605.

McCarter J, Bartlett B, Dang T, Schedl T (1999). On the control of oocyte meiotic maturation and ovulation in *Caenorhabditis elegans*. Dev Biol 205, 111–128.

McNally FJ, Vale RD (1993). Identification of katanin, an ATPase that severs and disassembles stable microtubules. Cell 75, 419–429.

McNally FJ, Thomas S (1998). Katanin is responsible for the M-phase microtubule-severing activity in Xenopus eggs. Mol Biol Cell 9, 1847–1861.

McNally K, Audhya A, Oegema K, McNally FJ (2006). Katanin controls mitotic and meiotic spindle length. J Cell Biol 175, 881–891.

McNally KP, Bazirgan OA, McNally FJ (2000). Two domains of p80 katanin regulate microtubule severing and spindle pole targeting by p60 katanin. J Cell Sci 113, 1623–1633.

Merdes A, Heald R, Samejima K, Earnshaw WC, Cleveland DW (2000). Formation of spindle poles by dynein/dynactin-dependent transport of NuMA. J Cell Biol 149, 851–862.

Pintard L *et al.* (2003). The BTB protein MEL-26 is a substrate-specific adaptor of the CUL-3 ubiquitin-ligase. Nature 425, 311–316.

Praitis V, Casey E, Collar D, Austin J (2001). Creation of low-copy intergrated transgenic lines in *Caenorhabditis elegans*. Genetics 157, 1217–1226.

Roll-Mecak A, McNally FJ (2010). Microtubule-severing enzymes. Curr Opin Cell Biol 22, 96–103.

Roll-Mecak A, Vale RD (2008). Structural basis of microtubule severing by the hereditary spastic paraplegia protein spastin. Nature 451, 363–367.

Scott A *et al.* (2005a). Structural and mechanistic studies of VPS4 proteins. EMBO J 24, 3658–3669.

Scott A, Gaspar J, Stuchell-Brereton MD, Alam SL, Skalicky JJ, Sundquist WI (2005b). Structure and ESCRT-III protein interactions of the MIT domain of human VPS4A. Proc Natl Acad Sci USA 102, 13813–13818.

Sharma N, Bryant J, Wloga D, Donaldson R, Davis RC, Jerka-Dziadosz M, Gaertig J (2007). Katanin regulates dynamics of microtubules and biogenesis of motile cilia. J Cell Biol 178, 1065–1079.

Srayko M, Buster DW, Bazirgan OA, McNally FJ, Mains PE (2000). MEI-1/MEI-2 katanin-like microtubule severing activity is required for Caenorhabditis elegans meiosis. Genes Dev 14, 1072–1084.

Stoppin-Mellet V, Gaillard J, Timmers T, Neumann E, Conway J, Vantard M (2007). Arabidopsis katanin binds microtubules using a multimeric microtubule-binding domain. Plant Physiol Biochem 45, 867–877.

Torres JZ, Miller JJ, Jackson PK (2009). High-throughput generation of tagged stable cell lines for proteomic analysis. Proteomics 9, 2888–2891.

Tsou MF, Hayashi A, DeBella LR, McGrath G, Rose LS (2002). LET-99 determines spindle position and is asymmetrically enriched in response to PAR polarity cues in *C. elegans* embryos. Development 129, 4469–4481.

Van Der Voet M, Berends CW, Perreault A, Nguyen-Ngoc T, Gönczy P, Vidal M, Boxem M, Van Den Heuvel S (2009). NuMA-related LIN-5, ASPM-1, calmodulin and dynein promote meiotic spindle rotation independently of cortical LIN-5/GPR/Galpha. Nat Cell Biol 11, 269–277.

Wignall SM, Villeneuve AM (2009). Lateral microtubule bundles promote chromosome alignment during acentrosomal oocyte meiosis. Nat Cell Biol 11, 839–844.

Yang HY, Mains PE, McNally FJ (2005). Kinesin-1 mediates translocation of the meiotic spindle to the oocyte cortex through KCA-1, a novel cargo adapter. J Cell Biol 169, 447–457.

Yang HY, McNally K, McNally FJ (2003). MEI-1/katanin is required for translocation of the meiosis I spindle to the oocyte cortex in C elegans. Dev Biol 260, 245–259.